Theoretical analysis of dynamic response of asymmetric dual quantum well lasers

Sotomitsu Ikeda
Canon Research Center, 5-1 Morinosato-Wakamiya, Atsugi-shi, Kanagawa 243-01, Japan

Akira Shimizu
Institute of Physics, The University of Tokyo, Komaba, Meguro-ku, Tokyo 153, Japan

(Received 9 March 1992; accepted for publication 16 June 1992)

Dynamic responses of the photon and carrier densities in an asymmetric dual quantum well laser which exhibits wavelength switching are analyzed theoretically. The laser consists of two different quantum wells isolated by a high and/or thick barrier layer that results in an inhomogeneous carrier injection into the two wells. The calculated pulse response at a voltage of the dual-wavelength lasing shows that the emission of the shorter wavelength light precedes that of the longer wavelength light by a nanosecond, in agreement with recent experimental results.

Monolithic laser diodes (LDs) which change the wavelength λ with a wide variable range $\Delta\lambda$ and/or emit multiple-wavelength light are required for future optoelectronic applications. As a new LD with these functions, we previously proposed an asymmetric dual quantum well (ADQW) LD,[1-5] for which we theoretically discussed static properties[2] and experimentally demonstrated the *discrete* switchings of $\Delta\lambda=13$ nm[3] and 50 nm[4] and *quasicontinuous* wavelength tuning of $\Delta\lambda=22$ nm,[5] when $\lambda\simeq 800$ nm. In this letter, we analyze pulse responses of photon and carrier densities in ADQW LDs.

The ADQW LD consists of two quantum wells, well 1 and well 2, of different emission wavelengths, λ_1 and λ_2 ($<\lambda_1$), respectively. The two wells are located in the core of a *single* optical waveguide, as shown in Fig. 1, where well 2 of a wider band gap is located on the p-type side.[2,4] If well 2 is located on the n-type side,[3,5] roles of the electrons and holes should be interchanged in the following discussions.

The point is to control the height and thickness of the barrier layer in such a way that holes are injected into the two wells inhomogeneously, and electrons homogeneously. From experimental results using various types of ADQW structure, we have found that it is easier to inject electrons homogeneously than holes. This is probably because the electron mobility is 20 times larger than that of holes. The holes injected from the p-type cladding layer are first trapped in well 2, and they are then thermally activated to be transferred over the barrier into well 1. By blocking this transfer with the high and/or thick barrier, the rate of the transfer can become comparable with the recombination rate. This should be contrasted with normal multiple-quantum well (MQW) LDs, for which barrier layers are usually too low and thin to inject carriers uniformly across many wells.[6] If we used such a low and thin barrier in an ADQW LD, most injected carriers would occupy well 1 only, so that the carrier density n_2 of well 2 would not reach the threshold density at a reasonable value of the injection current.[7] As for electrons, the sufficient electron densities are homogeneously distributed in both wells, as described above. Once the sufficient electron densities are thus obtained in both wells, we can focus on holes and photons, for which we can write down the following rate equations.[2] Although it is straightforward to extend the theory to include rate equations of electrons, we consider that main physics can be understood by the present simple equations.

When the component of the hole current which is *directly* injected into well 1 is zero, the set of rate equations for hole densities n_1, n_2 in well 1, well 2, respectively, and the photon densities s^{λ_1}, s^{λ_2} of the lasing modes at λ_1, λ_2 are given by[2]

$$\frac{dn_1}{dt}=\frac{J_{21}(n_1,n_2)}{ed_1}-G_1^{\lambda_1}(n_1)s^{\lambda_1}-G_1^{\lambda_2}(n_1)s^{\lambda_2}-\frac{n_1}{\tau_{n_1}}, \tag{1}$$

$$\frac{dn_2}{dt}=\frac{J-J_{21}(n_1,n_2)}{ed_2}-G_2^{\lambda_2}(n_2)s^{\lambda_2}-\frac{n_2}{\tau_{n_2}}, \tag{2}$$

$$\frac{ds^{\lambda_1}}{dt}=G_1^{\lambda_1}(n_1)s^{\lambda_1}-\frac{s^{\lambda_1}}{\tau^{\lambda_1}}+\beta_1^{\lambda_1}\frac{n_1}{\tau_{n_1}}, \tag{3}$$

$$\frac{ds^{\lambda_2}}{dt}=[G_1^{\lambda_2}(n_1)+G_2^{\lambda_2}(n_2)]s^{\lambda_2}-\frac{s^{\lambda_2}}{\tau^{\lambda_2}}+\beta_1^{\lambda_2}\frac{n_1}{\tau_{n_1}}+\beta_2^{\lambda_2}\frac{n_2}{\tau_{n_2}}, \tag{4}$$

where J_{21} is the hole-current density from well 2 to 1, τ_{n_1} and τ_{n_2} are the recombination lifetimes in well 1 and 2, respectively, and τ^{λ_1} and τ^{λ_2} are the lifetimes of the λ_1 and λ_2 photons. The $G_1^{\lambda_1}$, $G_1^{\lambda_2}$, and $G_2^{\lambda_2}$ ($\beta_1^{\lambda_1}$, $\beta_1^{\lambda_2}$, and $\beta_2^{\lambda_2}$) denote the optical gain coefficients (the spontaneous emission

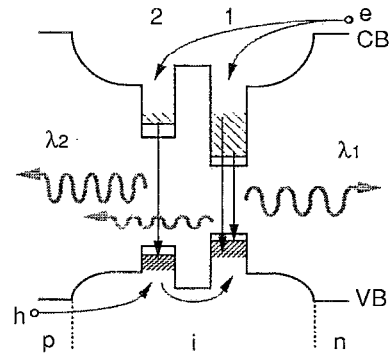

FIG. 1. A schematic band diagram of an ADQW LD. The shaded regions in the wells indicate the accumulated carriers.

 0003-6951/92/341016-03$03.00

factors) of λ_1 from well 1, λ_2 from well 1, and λ_2 from well 2, respectively. As for J_{21}, we here assume the following simple form:[2]

$$J_{21} \simeq e v n_2, \tag{5}$$

where v is the *effective* velocity of holes moving over the barrier.[8] The barrier must be high and/or thick enough so that v becomes much slower than that in normal MQW LDs.[8]

We assume, as usual, that $\beta_1^{\lambda_2}$ and $\beta_2^{\lambda_2}$ are constant, independent of the light intensity. On the other hand, $\beta_1^{\lambda_1}$ of ADQW LDs is expected to be an increasing function of s^{λ_2}. This is because the λ_2 photons will induce the *simultaneous* emission of the λ_1 photon and another quantum of energy $\hbar\omega_{21} \equiv \hbar\omega_2 - \hbar\omega_1$. The quantum may be either a phonon (the usual Raman process)[9] or a photon (the electronic Raman process).[9] In particular, the electronic Raman process becomes resonantly enhanced as $\hbar\omega_{21}$ approaches the intersubband level separation in well 1, as in the case of the sample of Ref. 4. Both types of the Raman processes will modify $\beta_1^{\lambda_1}$ into the following form:

$$\beta_1^{\lambda_1} = \beta_{10}^{\lambda_1} + \zeta^{\lambda_1} s^{\lambda_2}, \tag{6}$$

where the first term in the right-hand side is the usual term, and the second represents the Raman processes. It is very hard to estimate the coefficient ζ^{λ_1} from the first principles, because it requires detailed information on level broadening, phase matching conditions, and so on. We therefore treat ζ^{λ_1} as a fitting parameter.

A similar form to Eq. (6) is expected in usual LDs when an *external light* whose wavelength is close to the lasing wavelength is injected into the LD.[10] In our case of ADQW LDs, however, the λ_2 light is emitted from the LD *itself* and λ_2 is *much different* from the λ_1 light. In particular, s^{λ_2} is not an externally given parameter, but a variable which should be determined by solving the coupled rate Eqs. (1)–(4). That is, the whole situation is quite unique to ADQW LDs. Nevertheless, we can still expect from the knowledge about usual LDs that the spontaneous emission factor of the above form would reduce the relaxation oscillation of the λ_1 light. We will see below that this is indeed the case.

The optical gains are assumed to be of the usual form;[11,12]

$$G_1^{\lambda_1}(n_1) = g_a(n_1 - f_a), \tag{7}$$

$$G_2^{\lambda_2}(n_2) = g_b(n_2 - f_b), \tag{8}$$

where g_a, g_b are constants, and f_a, f_b are the inversion required to overcome the bulk losses. To simplify the calculation, we further assume that $G_1^{\lambda_2}(n_1) = \alpha G_1^{\lambda_1}(n_1)$, where α is a constant. Following Ref. 2, we define the threshold hole densities $n_{1\text{th}}$ and $n_{2\text{th}}$ by

$$G_1^{\lambda_1}(n_{1\text{th}}) = \frac{1}{\tau^{\lambda_1}}, \tag{9}$$

$$G_2^{\lambda_2}(n_{2\text{th}}) = \frac{1}{\tau^{\lambda_2}} - G_1^{\lambda_2}(n_{1\text{th}}). \tag{10}$$

TABLE I. The values of parameters used in the analysis.

Parameter	Value
ξ	0
d_2/d_1	1.35
$J_{\text{th}}^{\lambda_2}/J_{\text{th}}^{\lambda_1}$	2
$n_{2\text{th}}/n_{1\text{th}}$	0.5
τ_{n_1}	10^{-9} s
τ_{n_2}	10^{-9} s
τ^{λ_1}	10^{-12} s
τ^{λ_2}	10^{-12} s
$\tau_{n_1} g_a f_a$	10
$\tau_{n_2} g_b f_b$	10
α	0.4
$\beta_{10}^{\lambda_1}$	5×10^{-3}
$\beta_1^{\lambda_2}$	5×10^{-3}
$\beta_2^{\lambda_2}$	5×10^{-3}
$\zeta^{\lambda_1} n_{2\text{th}}$	1

Equations (7) and (8) can then be expressed as[12]

$$G_1^{\lambda_1}(n_1) = \frac{n_1 - n_{1\text{th}}}{n_{1\text{th}}}\left(\frac{1}{\tau^{\lambda_1}} + g_a f_a\right) + \frac{1}{\tau^{\lambda_1}}, \tag{11}$$

$$G_2^{\lambda_2}(n_2) = \frac{n_2 - n_{2\text{th}}}{n_{2\text{th}}}\left(\frac{1}{\tau^{\lambda_2}} - G_1^{\lambda_2}(n_{1\text{th}}) + g_b f_b\right) + \frac{1}{\tau^{\lambda_2}} - G_1^{\lambda_2}(n_{1\text{th}}). \tag{12}$$

To solve Eqs. (1)–(4) numerically, the Runge–Kutta method is used. The injection current J is assumed to be a rectangular pulse of height J_p and width $3\tau_{n_1}$, starting at $t=0$. The values of parameters used in the calculation are summarized in Table I.

Pulse responses of s^{λ_1}, s^{λ_2} and n_1, n_2 at $J_p = 1.2\, J_{\text{th}}^{\lambda_2}$ are shown in Figs. 2(a) and 2(b), respectively. The lasing of the λ_2 light with a relaxation oscillation starts nearly half a nanosecond before the slow start of the λ_1 lasing, as seen in Fig. 2(a), and the λ_2 lasing abruptly stops before the delayed end of the λ_1 lasing at the pulse end. These features of the lasing correspond with the change of carrier densities in the two wells in Fig. 2(b). The n_2 first reaches the threshold $n_{2\text{th}}$, and then the n_1 reaches the $n_{1\text{th}}$. At the pulse end, the n_2 decreases abruptly, whereas the n_1 decreases more slowly than that in conventional LDs. The *delayed* start and end of the λ_1 lasing is due to the reduced transport rate of holes from well 2 to well 1. Note that the λ_1 light exhibits weaker relaxation oscillation than the λ_2. We confirmed, by changing the value of ζ^{λ_1}, that this is due to the Raman process, as mentioned above.

With changing the J_p, the lasing behavior for each wavelength varies, as shown in Fig. 3. When $J_{\text{th}}^{\lambda_1} < J_p < J_{\text{th}}^{\lambda_2}$ [Fig. 3(a)], small s^{λ_1} starts with a weak relaxation oscillation after a long turn-on delay, and the steady part of s^{λ_2} is zero. These features agree with experimental results.[4] On the other hand, we experimentally observed a spike of the λ_2 light just before the emission of the λ_1.[4] Such a spike

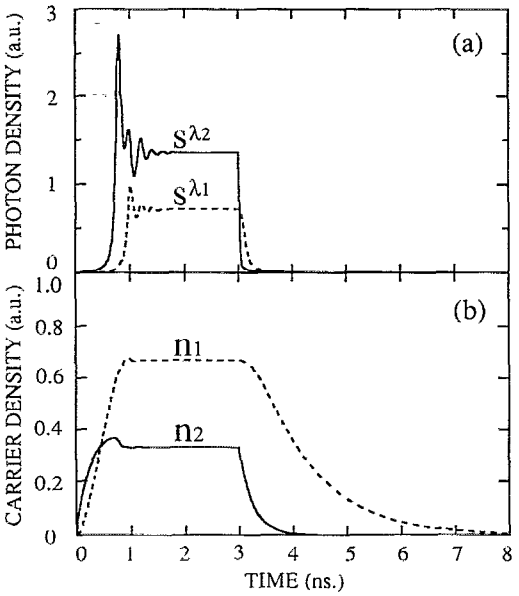

FIG. 2. Pulse responses of (a) the photon densities for the λ_1 (dashed line) and λ_2 light (solid line), and (b) carrier densities in well 1 (dashed line) and well 2 (solid line), respectively. The pulse height J_p of the injection current density is assumed to be 1.2 $J_{th}^{\lambda 2}$.

is absent from the present result. The cause of the discrepancy is under investigation at this stage.

When $J_p \gg J_{th}^{\lambda 2}$ [Fig. 3(b)], $s^{\lambda 2}$ becomes strong while $s^{\lambda 1}$ is suppressed. The pulse shape of the λ_2 light is like that from the normal LDs. As for the λ_1 light, on the other hand, a peak appears at the pulse end, unlike normal LDs, in agreement with experimental results.[4] This peak occurs because after J_p becomes zero, J_{21} (which lasts for a short time) is converted to $s^{\lambda 1}$ only, whereas while $J_p > 0$, J_{21} is converted to both $s^{\lambda 1}$ and $s^{\lambda 2}$.

Figure 4 plots the steady intensities at the latter part of

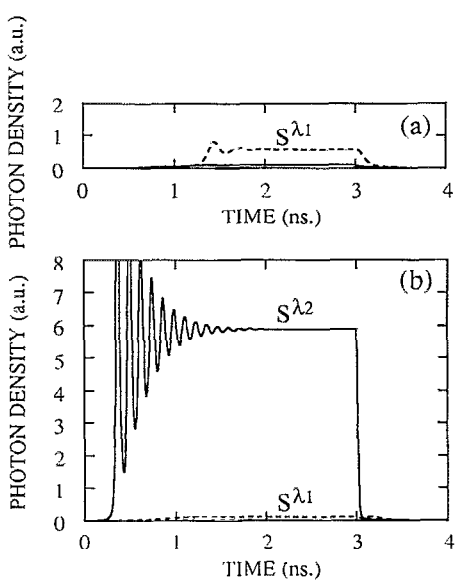

FIG. 3. Pulse responses of the photon densities for λ_1 (dashed line) and λ_2 (solid line) at (a) $J_p = 0.8\ J_{th}^{\lambda 2}$ and (b) $J_p = 2.0\ J_{th}^{\lambda 2}$, respectively.

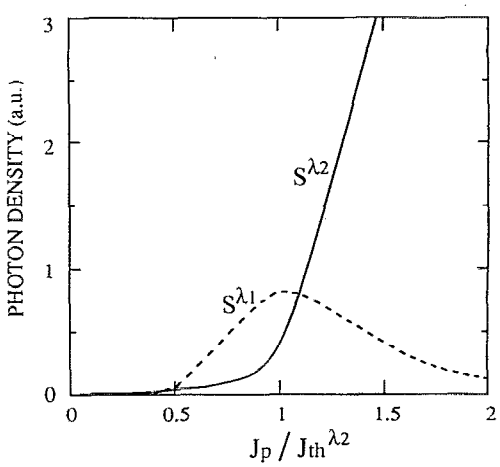

FIG. 4. Photon densities of the λ_1 (dashed line) and λ_2 light (solid line) at the steady part of the optical pulses are shown as a function of the pulse height of the injection current density.

the optical pulses, which correspond to those under cw operation, as a function of J_p. The lasing wavelength switches from λ_1 to λ_2 with increasing J_p, as expected from the static analysis.[2] The mechanism of the static switching was discussed in the previous letters.[2-4]

In the present analysis, we have assumed zero-bias current. We have also studied the bias-current dependence of the lasing characteristics. It is found that the time difference between the λ_1 and λ_2 lasing becomes short with increasing J_p, in agreement with experimental results.

In conclusion, we have analyzed the dynamic response of photon and carrier densities with basic Eqs. (1)–(4) of ADQW LDs. The numerical analysis shows the lasing of λ_2 starts a nanosecond before the slow start of λ_1 lasing, in agreement with recent experimental results. This lasing time lag occurs because the high and/or thick barrier between two wells of different emission wavelengths blocks the carrier transport between the wells.

The authors would like to thank Dr. Y. Handa and Dr. J. Nitta for valuable discussions.

[1] A. Shimizu, Jpn. Patents, JP63-211786 (1988) and JP63-211787 (1988).
[2] A. Shimizu and S. Ikeda, Appl. Phys. Lett. **59**, 765 (1991).
[3] S. Ikeda, A Shimizu, and T. Hara, Appl. Phys. Lett. **55**, 1155 (1989).
[4] S. Ikeda and A. Shimizu, Appl. Phys. Lett. **59**, 504 (1991).
[5] S. Ikeda, A. Shimizu, Y. Sekiguchi, M. Hasegawa, K. Kaneko, and T. Hara, Appl. Phys. Lett. **55**, 2057 (1989).
[6] W. T. Tsang, Appl. Phys. Lett. **39**, 786 (1981).
[7] Y. Toduda, T. Matsui, K. Fujiwara, N. Tsukada, and T. Nakayama, Appl. Phys. Lett. **51**, 209 (1987).
[8] The current J_{21} is carried by carriers, located in well 2, whose energies are higher than the barrier potential. Hence, $J_{21} \simeq ev_0 \delta n_2$, where δn_2 denotes the density of these high-energy carriers, and v_0 their average velocity. We can rewrite this in the form $J_{21} \simeq evn_2$, where $v \equiv v_0 \delta n_2 / n_2$, which we call the effective velocity. By using a high barrier, we can make $\delta n_2 \ll n_2$, and thus $v \ll v_0$. A typical value of v is $\sim 10^3$ cm/s, as mentioned in Ref. 2.
[9] See, e.g., Y. R. Shen, *The Principles of Nonlinear Optics* (Wiley, New York, 1984).
[10] R. Lang and K. Kobayashi, IEEE J. Quantum Electron. **QE-12**, 194 (1976).
[11] G. J. Lasher, Solid-State Electron. **7**, 707 (1964).
[12] T. Ikegami and Y. Suematsu, Trans. IECE Jpn. **51-B**, 57 (1968).